

École doctorale n° 364 : Sciences Fondamentales et Appliquées

## Doctorat ParisTech

### THÈSE

pour obtenir le grade de docteur délivré par

**l'École Nationale Supérieure des Mines de Paris**

**Spécialité doctorale “Science et Génie des Matériaux”**

*présentée et soutenue publiquement par*

**Ali SAAD**

le 26 avril 2015

## NUMERICAL MODELLING OF MACROSEGREGATION INDUCED BY SOLIDIFICATION SHRINKAGE IN A LEVEL SET APPROACH

Directeurs de thèse: **Michel BELLET**  
**Charles-André GANDIN**

### Jury

<b>M. Vincent Vega,</b>	Professeur, MINES ParisTech	Rapporteur
<b>M. Jules Winnfield,</b>	Professeur, Arts Et Métiers ParisTech	Rapporteur
<b>M. Butch Coolidge,</b>	Chargé de recherche, ENS Cachan	Examinateur
<b>Mme. Mya Wallace,</b>	Danseuse, en freelance	Examinateur
<b>M. Marsellus Wallace,</b>	Ingénieur, MIT	Examinateur

T  
H  
E  
S  
S



# Contents

<b>1 General Introduction</b>	<b>1</b>
1.1 Casting defects . . . . .	2
1.2 Macrosegregation . . . . .	3
1.2.1 Causes . . . . .	4
1.2.2 Types . . . . .	5
1.3 Industrial Worries . . . . .	7
1.4 Project context and objectives . . . . .	8
1.4.1 Context . . . . .	8
1.4.2 Objectives and outline . . . . .	9
<b>2 Modelling Review</b>	<b>11</b>
2.1 Introduction . . . . .	12
2.2 Modelling macrosegregation . . . . .	12
2.2.1 Dendritic growth . . . . .	12
2.2.2 Mush permeability . . . . .	13
2.2.3 Microsegregation . . . . .	14
2.2.4 Macroscopic solidification model: monodomain . . . . .	16
2.3 Motion description . . . . .	17
2.3.1 Langrangian description . . . . .	17
2.3.2 Eulerian description . . . . .	17
2.3.3 Arbitrary Langrangian-Eulerian . . . . .	17
2.4 Solidification models with level set . . . . .	18
2.5 The level set method (LSM) . . . . .	18
2.5.1 Transport and reiniliaztion . . . . .	18
2.5.2 Interface Remeshing . . . . .	18
2.5.3 Mixing Laws . . . . .	18
<b>Bibliography</b>	<b>19</b>

## **Contents**

---

---

<b>Acronym</b>	<b>Standing for</b>
ALE	Arbitrary Lagrangian-Eulerian
CCEMLCC	Chill Cooling for the Electro-Magnetic Levitator in relation with Continuous Casting of steel
CEMEF	Center for Material Forming
DLR	Deutsches Zentrum für Luft- und Raumfahrt
EML	Electromagnetic levitation
ESA	European Space Agency
ISS	International Space Station
IWT	Institut für Werkstofftechnik
RUB	Ruhr Universität Bochum
RVE	Representative Elementary Volume

---

## **Contents**

---

# Chapter 1

## General Introduction

**Macrosegregation** is a very known defect to metallurgical processes. Despite a great evolution achieved by active research during the last 60 years, it remains partially understood. Macrosegregation is often the consequence of several factors at the scale of a casting, all related to *microsegregation* happening at the scale of dendrites. Today, research in metallurgy focuses on a deeper understanding of such a connection between the different physical scales. Solidification is not only a phase change, but also a complex transformation involving small scales like nucleation, medium scales like grains growth and large scales like convection in the melt. From the nucleation theory to the mechanical behavior of metals, intricate phenomena combine to form defects in the final product. This has been seen in casting processes, such as continuous casting (fig. 1.1) and ingot casting. Surface and volume porosity, hot tearing and composition heterogeneity are known defects to the casting community. After a brief introduction of these defects, macrosegregation will be the focus of this dissertation.



Fig. 1.1 – Main steps in a continuous casting plant

## 1.1 Casting defects

Undesired effects are inevitable in any industrial process. More importantly, a lot of defects in the casting industry can be disastrous in some situations where the cast product is not serviceable and hence rejected. This leads to a systematic product recycling, i.e. the product is ditched to be reheated, remelted and then cast again. From an economic point view, the operation is expensive timewise and profitwise. Understanding and preventing defects when possible, is thus crucial in the casting industry. We focus hereafter on the main encountered defects.

### Hot tearing

This defect, also denoted solidification cracking or hot cracking, occurs in the mushy zone at high solid fractions when a failure or crack appears at specific locations, the hot spots. The temperature range in which the steel is vulnerable to hot tearing is known as the brittleness temperature range (BTR). It corresponds to solid fractions greater than 90%, with the liquid phase forming a discontinuous film. Many factors can cause the failure, but the main origin is a lack of liquid feeding required to compensate for the solidification shrinkage, in the presence of thermal stresses in the mushy region. Therefore, a crack initiates then propagates in the casting, as shown in [fig. 1.2](#).



**Fig. 1.2 – Crack in an aluminium slab**

### Porosity

Porosity is a void defect formed inside the casting or at the outer surface. It may attributed to two different factors. Firstly, we speak of *shrinkage porosity*, when a void forms as a result of density differences between the interdendritic liquid and solid network, the latter being denser than the former ([figs. 1.3c and 1.3d](#)). It is basically, the same reason that initiates hot cracks. The second factor is the presence of dissolved gaseous phases in the melt ([figs. 1.3a and 1.3b](#)). According to [Dantzig et al. \[2009\]](#), these gases may be initially in the melt, or created by the reaction between the metal and water found in the air or at trapped in grooves at the moulds surface. If the decreasing temperature and pressure drop in the liquid are large

enough, the latter becomes supersaturated. Consequently, the nucleation of gaseous phase is triggered (just like when you open a cold bottle of coca-cola is opened!).



**Fig. 1.3 – Examples of porosity in casting and welding**

### Freckles or segregated channels

The origin of this defect is a combined effect of microsegregation and buoyancy forces. Upon solidification, solid forms while rejecting some solute in the liquid due to partitioning (steels have a partition coefficient less than unity). When segregated solute is the lighter species, an increasing concentration in the liquid phase produces a solutal driving force inside the mushy zone, generating unstable convection currents, with "plume" shapes as often reported in the literature [Sarazin et al. 1992; Schneider et al. 1997; Shevchenko et al. 2013]. When temperature gradient is an additional force of convection, the latter is hence qualified as "thermosolutal".

## 1.2 Macrosegregation

Macrosegregation generally stems from a solubility difference between a liquid phase and one or more solid phases, along with a relative velocity between these phases. While the former is responsible for local solute enrichment or depletion, the latter will propagate the composition heterogeneity on a scale much larger than just a few dendrites. This is why macrosegregation could be observed on the scale of a casting, up to several meters in length.

While microsegregation can be healed by annealing the alloy to speed up the diffusion process and allow homogenization, heterogeneities spanning on larger distances cannot be treated after solidification. It is obvious that macrosegregation is irreversible defect. Failure to prevent it may lead to a substantial decline in the alloy's mechanical behavior, hence its serviceability.

### 1.2.1 Causes

Four main factors can (simultaneously) cause fluid flow leading to macrosegregation:

#### Liquid dynamics

During solidification, thermal and solutal gradients result in density gradients in the liquid phase:

$$\rho^l = \rho_{\text{ref}}(1 - \beta_T(T - T_{\text{ref}}) - \sum_i \beta_{\langle w_i \rangle^l}(\langle w_i \rangle^l - \langle w_i \rangle_{\text{ref}}^l)) \quad (1.1a)$$

$$\vec{\nabla} \rho^l = -\rho_{\text{ref}}(\beta_T \vec{\nabla} T + \sum_i \beta_{\langle w_i \rangle^l} \vec{\nabla} \langle w_i \rangle^l) \quad (1.1b)$$

In eq. (1.1a), density is assumed to vary linearly with temperature and phase composition for each chemical species (index  $i$ ). The slopes defining such variations are respectively the thermal expansion coefficient  $\beta_T$  and solutal expansion coefficient  $\beta_{\langle w_i \rangle^l}$ , given by [Kohler 2008]:

$$\beta_T = -\frac{1}{\rho_{\text{ref}}} \left( \frac{\partial \rho^l}{\partial T} \right) \quad (1.2a)$$

$$\beta_{\langle w_i \rangle^l} = -\frac{1}{\rho_{\text{ref}}} \left( \frac{\partial \rho^l}{\partial \langle w_i \rangle^l} \right) \quad (1.2b)$$

The linear fit assumes also that the density takes a reference value,  $\rho_{\text{ref}}$ , when temperature and liquid composition reach reference values, respectively  $T_{\text{ref}}$  and  $\langle w_i \rangle_{\text{ref}}^l$ . However, in some situations, a suitable thermodynamic database providing accurate density values is far better than a linear fit, especially in the current context of macrosegregation. Such possibility will be discussed later in the manuscript (cf. SECTION TODO ) In the presence of gravity, the density gradient in eq. (1.1b), causes thermosolutal convection in the liquid bulk and a subsequent macrosegregation.

#### Solidification shrinkage

Solid alloys have a greater density than the liquid phase ( $\rho^s > \rho^l$ ), thus occupy less volume. Upon solidification, the liquid moves towards the solidification front to compensate for the volume difference caused by the phase change, as well as the thermal contraction. When macrosegregation is triggered by solidification shrinkage, we speak of *inverse segregation*. Theoretically, if solute mass is conserved, a decreasing volume results in a positive segregation. Shrinkage deforms the outer surface of a solidifying alloy, causing positive macrosegregation.

While one would naturally expect negative macrosegregation in areas where solidification begins and positive inside the alloy, shrinkage promotes the opposite phenomenon, hence the term *inverse segregation*. In contrast to liquid convection, shrinkage flow may cause macrosegregation even without gravity.

### Movement of equiaxed grains

Equiaxed grains can grow in the liquid bulk where thermal gradients are weak, or in the presence of inoculants. Consequently, they are transported by the flow (floating or sedimenting, depending on their density [Beckermann 2002]) which leads to negative macrosegregation in their final position.

### Solid deformation

Stresses of thermal and mechanical nature are always found in casting processes (e.g. bulging between rolls in continuous casting). Deformation of the semi-solid in the mushy zone causes a relative solid-liquid flow in the inward (tensile stresses) or outward (compression stresses) direction, causing macrosegregation.

#### 1.2.2 Types

##### In continuous casting

The semi-solid billet is carried through a series of rolls that exert a radial force to straighten it and get it to its horizontal position. As the mushy part of a slab enters through these rolls, interdendritic liquid is expelled backwards, i.e. regions with lower solid fraction. Since the boundaries solidify earlier than the centre, the enriched liquid accumulates halfway in thickness, forming a centreline macrosegregation as shown in fig. 1.4. Other types of segregates (channels, A-segregates ...) can also be found but remain more specific to ingot casting.

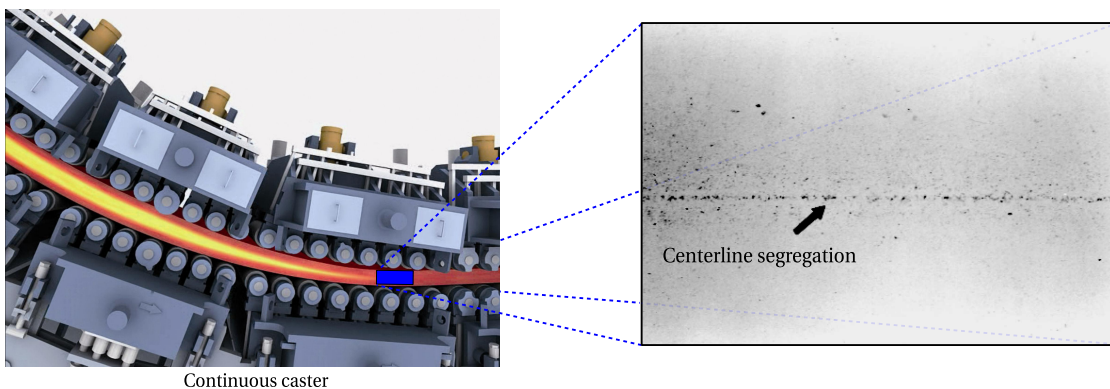


**Fig. 1.4 – Centreline segregation in a steel slab [Beckermann 2002]**

### In ingot casting

A variety of segregation patterns can be encountered in heavy ingots:

- the lower part is characterized by a negative segregation cone promoted by the sedimentation of equiaxed crystals,
- positive segregation channels, known as A-segregates, form along the columnar dendritic zones, close to the vertical contact with the mould,
- positive V-segregates can be identified in the centre of the ingot,
- a positive macrosegregation in the upper zone where the last liquid solidifies, the so-called "hot-top", caused by solidification shrinkage (inverse segregation) and thermosolutal buoyancy forces.

Combeau et al. [2009] state that A-segregates and V-segregates formation is mainly attributed to local flow phenomena. As such, their scale is finer than macrosegregation, hence called "mesosegregates".



**Fig. 1.5** – Sulphur print (left) of a 65-ton steel ingot [Lesoult 2005] showing various patterns (right) of macrosegregation [Flemings 1974]

### In investment casting

This process is widely used to cast single-crystal (SC) alloys for turbines and other applications that require excellent mechanical behavior [Giamei et al. 1970]. During directional solidification, thermosolutal forces thrust segregated species outside of the mushy zone into the liquid bulk. The segregation scale ranges from a few dendrites to a few hundreds of them, hence forming "long and narrow trails" (fig. 1.6a) as described by Felicelli et al. [1991]. Freckles are frequently formed by small equiaxed grains (fig. 1.6b), probably caused by a uniform temperature gradient that settles as the channels become richer in solute. They can be observed on the ingot's surface, as well as in the volume.

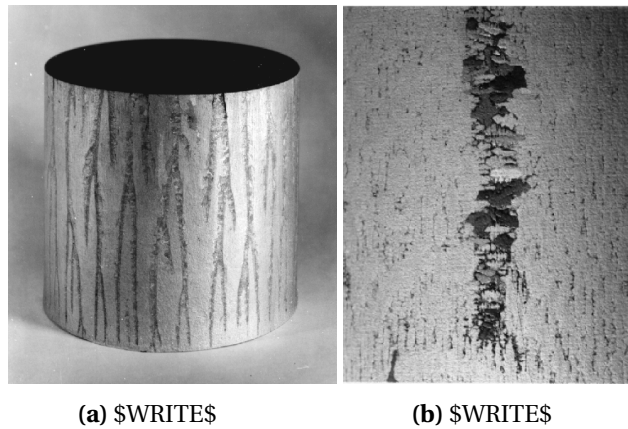


**Fig. 1.6** – Freckles in directional casting of nickel-base superalloys

### 1.3 Industrial Worries

**Steel production** has continuously increased over the years to meet the industrial needs. [Figure 1.7](#) shows this increase between 1980 and 2013 with a clear dominance of the Chinese production. Quality constraints have also increased where specific grades of steel are needed in critical applications such as mega-structures in construction and heavy machinery. Therefore, alloys with defects are considered vulnerable and should be avoided as much as possible during the casting process. As such, steelmakers have been investing in research, with the aim of understanding better the phenomena leading to casting problems, and improve the processes when possible.



**Fig. 1.7** – Evolution curves of crude steel worldwide production from 1980 to 2013

**Simulation software** dedicated to alloy casting is one of the main research investments undertaken by steelmakers. These tools coming from academic research are actively used to optimize the process. However, few are the tools that take into account the casting environ-

## **Chapter 1. General Introduction**

---

ment. For instance, the continuous casting process, in [fig. 1.1](#), is a chain process where the last steps involve rolls, water sprays and other components. A dedicated software is one that can provide the geometric requirements with suitable meshing capabilities, as well as respond to metallurgical and mechanical requirements, mainly:

- handling moulds and their interaction with the alloy (thermal resistances ...)
- handling alloy filling and predicting velocity in the liquid and mushy zone
- handling thermomechanical stresses in the solid
- handling multicomponent alloys and predicting macrosegregation
- handling finite solute diffusion in solid phases
- handling real alloy properties (not just constant thermophysical/thermomechanical properties)

## **1.4 Project context and objectives**

### **1.4.1 Context**

The European Space Agency (ESA) has been actively committed, since its foundation in 1975, in the research field. Its covers not only exclusive space applications, but also fundamental science like solidification. This thesis takes part of the ESA project entitled *CCEMLCC*, abbreviating "Chill Cooling for the Electro-Magnetic Levitator in relation with Continuous Casting of steel". The three-year contract from 2011 to late 2014 denoted *CCEMLCC II*, was preceded by an initial project phase, *CCEMLCC I*, from 2007 to 2009. The main focus is studying containerless solidification of steel under microgravity conditions. A chill plate is later used to extract heat from the alloy, simulating the contact effect with a mould in continuous casting or ingot casting. A partnership of 7 industrial and academic entities was formed in *CCEMLCC II*. A brief summary of each partner's commitment:

#### **Academic partners**

- CEMEF (France): numerical modelling of microgravity chill cooling experiments
- DLR (German Aerospace Centre) and RUB university (Germany): preparation of a chill cooling device for electromagnetic levitation (EML), microgravity testing and investigation of growth kinetics in chill-cooled and undercooled steel alloys
- University of Alberta (Canada): impulse atomization of the D2 tool steel
- University of Bremen - IWT institute (Germany): study of melt solidification in atomization processing

#### **Industrial partners**

- ARCELORMITTAL (France): elaboration of a series of steel grades used in microgravity and ground studies

- METSO Minerals Inc. (Finland): material production with D2 tool steel for spray forming
- TRANSVALOR (France): development and marketing of casting simulation software *Thercast<sup>®</sup>*

CEMEF, as an academic partner, contributed to the work by proposing numerical models in view of predicting the chill cooling of steel droplets. A first model was developed by Rivaux [2011] whereas the present discusses a new model. The experimental work considered various facilities and environments to set a droplet of molten alloy in levitation: EML (fig. 1.8) for ground-based experiments, microgravity in parabolic flight or sounding rockets and last, microgravity condition on-board the International Space Station (ISS)

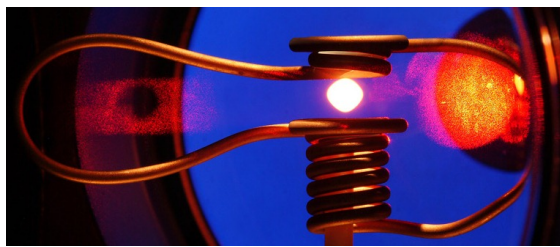


**Fig. 1.8 – Electromagnetic levitation**

### 1.4.2 Objectives and outline

The main focus of the present thesis is macrosegregation with liquid dynamics assuming a fixed solid phase, i.e. no account of solid transport (e.g. equiaxed crystals sedimentation) and no account of solid deformation. In CEMEF, this scope has been adopted for previous work by Gouttebroze [2005], Liu [2005], Mosbah [2008], Rivaux [2011], and Carozzani [2012]. Nevertheless, many modelling features evolved with time such as going from two-dimensional to three-dimensional modelling, resolution schemes for each of the conservation equations: energy, chemical species and liquid momentum, Eulerian or Lagrangian descriptions, modelling of grain structure and others. In this thesis, we propose a numerical model that takes into account i) the energy conservation in a temperature formulation based on a thermodynamic database mapping, ii) the liquid momentum conservation with thermosolutal convection and solidification shrinkage as driving forces, iii) solute mass conservation and iv) solidification paths at full equilibrium for multicomponent alloys microsegregation. Moreover, all equations are formulated in a pure Eulerian description while using the Level Set method to keep implicitly track of the interface between the alloy and surrounding gas. To the author's knowledge, this work combining macrosegregation prediction using the level set methodology to track the metal-air interface during shrinkage has no precedent in the literature.

*Numerical tools: Cimlib relying on PETSc, parallelized with MPICH2, paraview and python as tools for postprocess and analysis.*

*The previously mentionned simulation requirements are not met in a single casting software package. Nevertheless, Thercast<sup>®</sup> is a promising tool that already handles a part of the above*

## **Chapter 1. General Introduction**

---

*points. The current thesis developments are done using C++ language as a part of the in-house code, known as CimLib [Digonnet et al. 2007; Mesri et al. 2009]. This fully parallel library is the main academic research support for Thercast®.*

**Outline** Each chapter content

### **Biblio test**

Carozzani et al. [2013] is textual  
[Carozzani et al. 2013] is parenthetical

### **Cross reference test**

ref gives [1.2a](#)  
cref gives [eq. \(1.2a\)](#)  
Cref gives [Equation \(1.2a\)](#)  
autoref gives [Equation 1.2a](#)

ref gives [1.3a](#)  
cref gives [fig. 1.3a](#)  
Cref gives [Figure 1.3a](#)  
autoref gives [Figure 1.3a](#)

## Chapter 2

# Modelling Review

### Contents

---

<b>2.1</b>	<b>Introduction</b>	<b>12</b>
<b>2.2</b>	<b>Modelling macrosegregation</b>	<b>12</b>
2.2.1	Dendritic growth	12
2.2.2	Mush permeability	13
2.2.3	Microsegregation	14
2.2.4	Macroscopic solidification model: monodomain	16
<b>2.3</b>	<b>Motion description</b>	<b>17</b>
2.3.1	Langrangian description	17
2.3.2	Eulerian description	17
2.3.3	Arbitrary Langrangian-Eulerian	17
<b>2.4</b>	<b>Solidification models with level set</b>	<b>18</b>
<b>2.5</b>	<b>The level set method (LSM)</b>	<b>18</b>
2.5.1	Transport and reiniliaztion	18
2.5.2	Interface Remeshing	18
2.5.3	Mixing Laws	18

---

## 2.1 Introduction

Divide into 2 families of models: with and without level set. Regarding the second family of models, the level set method has been applied on several occasions, but in a different way. Some references apply it to track the solid-liquid interface, a situation more commonly known as the "Stefan problem". The scope such applications mainly encompasses dendritic modelling and simulation

### SOURCES:

<http://www.sciencedirect.com/science/article/pii/S0021999105002603>

<http://physbam.stanford.edu/~fedkiw/papers/stanford2002-04.pdf>

Other references, in relevance to our scope, apply this method to track the surface of the metal while going from the liquid state to the solid state, in contact with the surrounding gas which is usually air.

## 2.2 Modelling macrosegregation

### 2.2.1 Dendritic growth

In a casting process, the chill surface i.e. the contact between the molten alloy and relatively cold moulds, is the first area to solidify. Thermal gradient,  $G$ , and cooling rate  $R$  are two crucial process parameters that define the interface speed  $\vec{v}^*$ , which in turn, affects the initial microstructure. Although it may be not easy to control them, it remains important to understand their implication in solidification.

The solid-liquid interface fluctuates when solidifying, thus perturbations may appear on the front, locally destabilizing it. Two outcome scenarios are possible. The first scenario is characterized by low values of  $\vec{v}^*$  where the interface maintains a planar shape, hence we speak of *planar growth*. With this kind of growth, a random protuberance appearing at the interface, has a low tip velocity (low driving force of solidification). As such, the rest of the interface catches up, keeping the planar geometry. In another scenario, where a real casting is considered, the interface speed is greater in general, due to high solidification rate. The protuberance tip will be pulled into a liquid less rich in solute than the interface. The zone ahead of the solid-liquid interface is constitutionally undercooled [Tiller et al. 1953], giving a greater driving force for the protuberance to grow in the direction of the thermal gradient. As it has a tree-like shape, we speak of *dendritic growth*. Near the chill surface, dendrites are columnar, with a favourable growth in the  $<100>$  direction for alloys with cubic lattices, but different orientations are also reported in the literature [see Dantzig et al. 2009, p. 289]. If temperature is uniform, which the case usually far from mould walls, a similar dendritic growth phenomenon occurs, but with an equiaxed morphology.

Columnar dendrites are characterized by a primary spacing,  $\lambda_1$ , between the main trunks, and a secondary spacing,  $\lambda_2$ , for the arms that are perpendicular to the trunks. It should be noted that  $\lambda_2$ , together with the grain size, are two important microstructural parameters in the as-cast microstructure [Easton et al. 2011]. Further branching may occur but will not be discussed here.

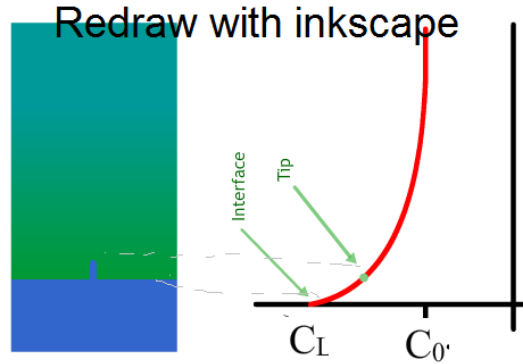


**Fig. 2.1** – Schematic of a) a protuberance growing on the solid-liquid interface with b) the corresponding composition profiles (Reproduced and adapted from [DoITPoMS \[2000\]](#), © DoITPoMS, University of Cambridge)

### 2.2.2 Mush permeability

The dendritic geometry is crucial in solidification theory as it exhibits lower solid fraction compared to a microstructure formed by planar growth. This fact has consequences in the fluid-structure interaction in the mushy zone, namely the liquid flow through dendrites. At the chill surface, the solid grows gradually from dispersed growing nuclei, to a permeable solid skeleton until finally grains have fully grown with the end of phase change. The intermediate state where liquid can flow in and out of the mushy zone through the dendrites is a key phenomenon from a rheological perspective. The flow through the solid skeleton is damped by primary and secondary dendrites, resulting in momentum dissipation just like in saturated porous media. The famous [Darcy \[1856\]](#) law relates the pressure gradient ( $\vec{\nabla} p$ ) to the fluid velocity  $\vec{v}$ , through the following equation [\[Rappaz et al. 2003\]](#):

$$\vec{v} = \frac{\mathbb{K}}{\mu} \vec{\nabla} p \quad (2.1)$$

where  $\mu$  is the liquid dynamic viscosity and  $\mathbb{K}$  is the permeability tensor. The latter parameter has been the subject of numerous studies that aimed to predict it from various microstructural or morphological parameters. Some of these studies have started even before the first attempts to model macrosegregation by [Flemings et al. \[1967\]](#), [Flemings et al. \[1968a\]](#), and [Flemings et al. \[1968b\]](#). Basically, all models include the solid fraction,  $g^s$ , as input to predict mush permeability along with empirical data. An instance of such models is the work of [Xu et al. \[1991\]](#). Some models rely additionally on the primary dendrite arm spacing  $\lambda_1$  like Blake-Kozeny [\[Ramirez et al. 2003\]](#), or the secondary dendrite arm spacing  $\lambda_2$  like Carman-Kozeny, as a meaningful parameter to determine an isotropic permeability. Other models like [Poirier \[1987\]](#) and [Felicelli et al. \[1991\]](#) derive an anisotropic permeability based on both  $\lambda_1$  and  $\lambda_2$ .

The present work uses Carman-Kozeny as a constitutive model for the permeability scalar

(zero order tensor):

$$\mathbb{K} = \frac{\lambda_2^2 g^{l^3}}{180(1 - g^l)^2} \quad (2.2)$$

### 2.2.3 Microsegregation

Microsegregation is a fundamental phenomenon in solidification. The simplest definition would be an uneven distribution of solute between liquid and the herein growing solid, at the microscopic scale of the interface separating these phases. If we consider a binary alloy, then the solubility limit is the key factor that dictates the composition at which a primary solid phase exists in equilibrium. The segregation (or partition) coefficient  $k$  determines the extent of solute rejection into the liquid during solidification:

$$k = \frac{w^{s^*}}{w^{l^*}} \quad (2.3)$$

where  $w^{s^*}$  and  $w^{l^*}$  are the compositions of the solid and liquid respectively, at the interface. When the segregation coefficient is less than unity (such is the case for most alloys during dendritic solidification), the first solid forms with a composition  $kw^{l^*} = kw_0$  less than the liquid's composition  $w_0$ , the latter being initially at the nominal composition,  $w_0$ . [Figure 2.2](#) illustrates a typical binary phase diagram where the real solidus and liquidus are represented by solid lines, while the corresponding linear approximations are in dashed lines. For most binary alloys, this linearisation simplifies derivation of microsegregation models, as  $k$  becomes independent of temperature.

For each phase, the relationship between the composition at the interface and that in the bulk depends on the chemical homogenisation ability of the phase. The more homogeneous a phase, the closer the concentrations between the interface and the bulk, hence closer to equilibrium. It is thus essential to study the effect of homogenisation on the segregation behaviour and the subsequent effect on solidification, which leads the formalism of microsegregation models.

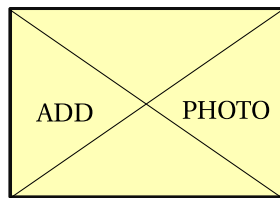


**Fig. 2.2 – Simplified binary phase diagram**

### Microsegregation models

Solid formation depends greatly on the ability of chemicals species to diffuse within each of the solid and liquid phases, but also across the solid-liquid interface. Furthermore, chemical

diffusion like all other diffusional process, is a time-dependent phenomenon. One can thus conclude that two factors influence the amount of solid formation: cooling rate and diffusion coefficients. However, convection and other mechanical mixing sources, homogenise the composition much faster than atomic diffusion. As such, *complete mixing* in the liquid is always an acceptable assumption, regardless of the solidification time. We may speak of infinite diffusion in the liquid. Nevertheless, diffusion in the solid also known as *back diffusion*, is the only transport mechanism with very low diffusion coefficients. Therefore, chemical species will need a lot of time, i.e. low cooling rate, before it can diffuse within the solid. The difference in diffusional behaviour is summarized by two limiting segregation models of perfect equilibrium and nonequilibrium at the scale of a secondary dendrite arm, which are the lever rule and Gulliver-Scheil models, respectively. Afterwards, models with finite back diffusion are presented.

### Lever rule

The lever rule considers an ideal equilibrium in all phases, i.e. solidification is extremely slow, hence phase compositions are homogeneous ( $w^{l*} = w^l$  and  $w^{s*} = w^s$ ) at all times as a consequence of complete mixing. These compositions are given by:

$$w^l = w^{l*} = kw^{s*} = kw^s \quad (2.4)$$

$$w^s = w^{s*} = \frac{w_0}{k(1 - f^s) + f^s} \quad (2.5)$$

At the end of solidification, the composition of the solid phase is equal to the nominal composition,  $w^s = w_0$

### Gulliver-Scheil

The other limiting case is the absence of diffusion in the solid. That includes also the diffusion at the interface, so nothing diffuses in or out. The consequence is a steady increase of the homogeneous liquid composition while the solid composition remains non-uniform. Compared to a full equilibrium approach, higher fractions of liquid will remain until eutectic composition is reached, triggering a eutectic solidification. The phase compositions are given by:

$$w^l = w^{l*} = kw^{s*} \quad (2.6)$$

$$w^s = kw_0(1 - f^s)^{1-k} \quad (2.7)$$

### Finite back diffusion

It has been concluded that the assumption of a negligible back diffusion overestimates the liquid composition and the resulting eutectic fraction. Therefore, many models studied the limited diffusion in the solid. One of the earliest models is the Brody-Flemings models [Khan et al. 2014] that is based on a differential solute balance equation for a parabolic growth rate,

as follows:

$$w^l = w^{l*} = kw^{s*} \quad (2.8)$$

$$w^s = kw_0 [1 - (1 - 2\text{Fo}^s k) f^s]^{\frac{k-1}{1-2\text{Fo}^s k}} \quad (2.9)$$

where  $\text{Fo}^s$  is the dimensionless *Fourier number* for diffusion in the solid [Dantzig et al. 2009]. It depends on the solid diffusion coefficient  $D^s$ , solidification time  $t_s$  and the secondary dendrite arm spacing, as follows:

$$\text{Fo}^s = \frac{D^s t_s}{(\lambda_2/2)^2} \quad (2.10)$$

Several other models were since suggested and used. The interested reader is referred to the following non exhaustive list of publications: Clyne et al. [1981], Kobayashi [1988], Ni et al. [1991], Wang et al. [1993], Combeau et al. [1996], Martorano et al. [2003], and Tourret et al. [2009].

#### 2.2.4 Macroscopic solidification model: monodomain

In this section, we will present the macroscopic conservations equations that enable us to predict macrosegregation in the metal when the latter is the only domain in the system.

##### Volume averaging

It is crucial for a solidification model to represent phenomena on the microscale, then scale up to predict macrscopic phenomena. Nevertheless, the characteristic length of a small scale in solidification may represent a dendrite arm spacing, for instance the mushy zone permeability, as it may also represent an atomic distance if one is interested, for instance, in the growth competition between diffusion and surface energy of the solid-liquid interface. Modelling infinitely small-scale phenomena could be prohibitively expensive in computation time, if the we target industrial scales.

The volume averaging is a technique that allows bypassing this barrier by averaging small-scale variations on a so-called *representative volume element* (RVE) [Dantzig et al. 2009] with the following dimensional constraints on its volume,  $V_E$ : the element should be large enough to "see" and average microscopic fluctuations whilst being smaller than the scale of macroscopic variations. Solid and liquid may exist simultaneously in the RVE, but no gas phase is considered (volume saturation:  $V^s + V^l = V_E$ ). Moreover, temperature is assumed uniform and equal for all the phases. The formalism, introduced by Ni et al. [1991], is summarized by the following equations for any physical quantity  $\psi$ :

$$\langle \psi \rangle = \frac{1}{V_E} \int_{V_E} \psi d\Omega = \langle \psi^s \rangle + \langle \psi^l \rangle \quad (2.11)$$

where  $\langle \psi \rangle^s$  and  $\langle \psi \rangle^l$  are phase averages of  $\psi$ . Then, for any phase  $\phi$ , one can introduce the

*phase intrinsic average* of  $\psi$ , denoted  $\langle \psi \rangle^\phi$ , by writing:

$$\langle \psi^\phi \rangle = \frac{1}{V_E} \int_{V^\phi} \psi \, d\Omega = g^\phi \langle \psi \rangle^\phi \quad (2.12)$$

where  $g^\phi$  is the volume fraction of the phase. To finalize, the averaging is applied to temporal and spatial derivation operators [Rivaux 2011]:

$$\langle \frac{\partial \psi^\phi}{\partial t} \rangle = \frac{\partial \langle \psi^\phi \rangle}{\partial t} - \int_{\Gamma^*} \psi^\phi \vec{v}^* \cdot \vec{n}^\phi \, d\Gamma \quad (2.13)$$

$$\langle \vec{\nabla} \psi^\phi \rangle = \vec{\nabla} \langle \psi^\phi \rangle + \int_{\Gamma^*} \psi^\phi \vec{n}^\phi \, d\Gamma \quad (2.14)$$

where  $\vec{v}^*$  is the local relative interface velocity and  $\Gamma^*$  is the solid-liquid interface, while  $\vec{n}^\phi$  is the normal to  $\Gamma^*$ , directed outwards. The previous equations will be used to derive a set macroscopic conservation equations. It is noted that the intrinsic average  $\langle \psi \rangle^\phi$  may be replaced by  $\psi^\phi$  for notation simplicity, whenever the averaging technique applies.

### Macroscopic equations

Macro models:

- Rivaux ?
- Gu beckermann 1999 ?

MICRO MACRO:

- Tommy Carozzani (direct)
- P. Thévoz, J.-L. Desbiolles, M. Rappaz, Metallurgical and Materials TransactionsA 20 (2) (1989) 311–322
- guo beckermann 2003
- Combeau 2009
- Miha Zaloznik 2010 (indirect)

end by talking about taking air into account and the need for an interface capturing method

## 2.3 Motion description

### 2.3.1 Langrangian description

### 2.3.2 Eulerian description

### 2.3.3 Arbitrary Langrangian-Eulerian

a little history [Hirt 1971]

The ALE method combines advantages from both previous descriptions. Explain how the

position mesh nodes can be updated with velocity or fixed. However, this description will be more suitable for configuration with deformable solid. Further discussions are presented in the perspectives.

## **2.4 Solidification models with level set**

Should I mention the use of level set in mould filling, which comes before solidification  
Talk about the models used for welding processes.

Pure MACRO models:

- Solidification: Du 2001 (double casting technique)
- Welding: olivier desmaison
- Welding: mickael from lorient

Aside from the welding applications, check these articles [http://www.tandfonline.com/doi/abs/10.1080/10407790050051137#.VF\\_gLvnF\\_kU](http://www.tandfonline.com/doi/abs/10.1080/10407790050051137#.VF_gLvnF_kU)  
[http://www.math.pku.edu.cn/pzhang/publication/2001\\_SDCTULSM.pdf](http://www.math.pku.edu.cn/pzhang/publication/2001_SDCTULSM.pdf)  
MESO MACRO: Shijia Chen (CAFE+LS)

## **2.5 The level set method (LSM)**

How it is defined, Heaviside, mixing laws, transport and reinitialization

in the article 2004SunBeckermann, in the introduction there is a small discussion about the importance of the diffuse interface thickness, check references 3 and 10

### **2.5.1 Transport and reinilaztion**

Strong and weak form of transport

Numerical stability

**Convective reinitialization and Hamilton-Jacobi equations**

**Geometric reinitialization**

### **2.5.2 Interface Remeshing**

Importance when using a static level set and more importantly when LS is transported, influence of mixing area *thickness* and *resolution* (i.e. nb of nodes with the area), Isotropic or anisotropic ? the first is more important to composition calculation while the second is more relevant if we mean do thermohydraulics without macrosegregation

### **2.5.3 Mixing Laws**

# Bibliography

## [Beckermann 2002]

Beckermann, C. (2002). "Modelling of macrosegregation: applications and future needs". *International Materials Reviews*, 47 (5), pp. 243–261. URL: <http://www.maneyonline.com/doi/abs/10.1179/095066002225006557> (cited on page 5).

## [Carozzani 2012]

Carozzani, T. (2012). "Développement d'un modèle 3D Automate Cellulaire-Éléments Finis (CAFE) parallèle pour la prédiction de structures de grains lors de la solidification d'alliages métalliques". PhD thesis. Ecole Nationale Supérieure des Mines de Paris. URL: <http://pastel.archives-ouvertes.fr/pastel-00803282> (cited on page 9).

## [Carozzani et al. 2013]

Carozzani, T. et al. (2013). "Direct Simulation of a Solidification Benchmark Experiment". *Metallurgical and Materials Transactions A*, 44 (2), pp. 873–887. URL: <http://link.springer.com/article/10.1007/s11661-012-1465-1> (cited on page 10).

## [Clyne et al. 1981]

Clyne, T. W. and W. Kurz (1981). "Solute redistribution during solidification with rapid solid state diffusion". *Metallurgical Transactions A*, 12 (6), pp. 965–971. URL: <http://link.springer.com/article/10.1007/BF02643477> (cited on page 16).

## [Combeau et al. 1996]

Combeau, H. et al. (1996). "Modeling of microsegregation in macrosegregation computations". *Metallurgical and Materials Transactions A*, 27 (8), pp. 2314–2327. URL: <http://link.springer.com/article/10.1007/BF02651886> (cited on page 16).

## [Combeau et al. 2009]

Combeau, H. et al. (2009). "Prediction of Macrosegregation in Steel Ingots: Influence of the Motion and the Morphology of Equiaxed Grains". *Metallurgical and Materials Transactions B*, 40 (3), pp. 289–304. URL: <http://link.springer.com/article/10.1007/s11663-008-9178-y> (cited on page 6).

## [Dantzig et al. 2009]

Dantzig, J. A. and M. Rappaz (2009). *Solidification*. EPFL Press (cited on pages 2, 12, 16).

## [Darcy 1856]

Darcy, H. (1856). *Les fontaines publiques de la ville de Dijon : exposition et application des principes à suivre et des formules à employer dans les questions de distribution d'eau*. V. Dalmont (Paris). URL: <http://gallica.bnf.fr/ark:/12148/bpt6k624312> (cited on page 13).

## Bibliography

---

### [Digonnet et al. 2007]

Digonnet, H. et al. (2007). "Cimlib: A Fully Parallel Application For Numerical Simulations Based On Components Assembly". *AIP Conference Proceedings*. Vol. 908. AIP Publishing, pp. 269–274. URL: <http://scitation.aip.org/content/aip/proceeding/aipcp/10.1063/1.2740823> (cited on page 10).

### [DoITPoMS 2000]

DoITPoMS (2000). *Dissemination of IT for the Promotion of Materials Science*. URL: <http://www.doitpoms.ac.uk/> (cited on page 13).

### [Easton et al. 2011]

Easton, M. et al. (2011). "Grain Morphology of As-Cast Wrought Aluminium Alloys". *Materials Transactions*, 52 (5), pp. 842–847 (cited on page 12).

### [Felicelli et al. 1991]

Felicelli, S. D. et al. (1991). "Simulation of freckles during vertical solidification of binary alloys". *Metallurgical Transactions B*, 22 (6), pp. 847–859. URL: <http://link.springer.com/article/10.1007/BF02651162> (cited on pages 6, 13).

### [Flemings 1974]

Flemings, M. C. (1974). "Solidification processing". *Metallurgical Transactions*, 5 (10), pp. 2121–2134. URL: <http://link.springer.com/article/10.1007/BF02643923> (cited on page 6).

### [Flemings et al. 1967]

Flemings, M. C. and G. E. Nereo (1967). "Macrosegregation: Part I". *Transactions of the Metallurgical Society of AIME*, 239, pp. 1449–1461 (cited on page 13).

### [Flemings et al. 1968a]

Flemings, M. C. et al. (1968a). "Macrosegregation: Part II". *Transactions of the Metallurgical Society of AIME*, 242, pp. 41–49 (cited on page 13).

### [Flemings et al. 1968b]

Flemings, M. C. and G. E. Nereo (1968b). "Macrosegregation: Part III". *Transactions of the Metallurgical Society of AIME*, 242, pp. 50–55 (cited on page 13).

### [Giamei et al. 1970]

Giamei, A. F. and B. H. Kear (1970). "On the nature of freckles in nickel base superalloys". *Metallurgical Transactions*, 1 (8), pp. 2185–2192. URL: <http://link.springer.com/article/10.1007/BF02643434> (cited on page 6).

### [Gouttebroze 2005]

Gouttebroze, S. (2005). "Modélisation 3d par éléments finis de la macroségrégation lors de la solidification d'alliages binaires". PhD thesis. École Nationale Supérieure des Mines de Paris. URL: <https://pastel.archives-ouvertes.fr/pastel-00001885/document> (cited on page 9).

### [Hirt 1971]

Hirt, C. W. (1971). "An arbitrary Lagrangian-Eulerian computing technique". *Proceedings of the Second International Conference on Numerical Methods in Fluid Dynamics*. Ed. by M. Holt. Lec-

- ture Notes in Physics 8. Springer Berlin Heidelberg, pp. 350–355. URL: [http://link.springer.com/chapter/10.1007/3-540-05407-3\\_50](http://link.springer.com/chapter/10.1007/3-540-05407-3_50) (cited on page 17).
- [Khan et al. 2014]**  
Khan, M. I. et al. (2014). “Influence of Cooling Rate on Microsegregation Behavior of Magnesium Alloys”. *Journal of Materials*, 2014, e657647. URL: <http://www.hindawi.com/journals/jma/2014/657647/abs/> (cited on page 15).
- [Kobayashi 1988]**  
Kobayashi, S. (1988). “Solute redistribution during solidification with diffusion in solid phase: A theoretical analysis”. *Journal of Crystal Growth*, 88 (1), pp. 87–96. URL: <http://www.sciencedirect.com/science/article/pii/S0022024898900100> (cited on page 16).
- [Kohler 2008]**  
Kohler, F. (2008). “Peritectic solidification of Cu-Sn alloys: microstructure competition at low speed”. PhD thesis. EPFL (cited on page 4).
- [Lesoult 2005]**  
Lesoult, G. (2005). “Macrosegregation in steel strands and ingots: Characterisation, formation and consequences”. *Materials Science and Engineering: A*, International Conference on Advances in Solidification Processes 413–414, pp. 19–29. URL: <http://www.sciencedirect.com/science/article/pii/S0921509305010063> (cited on page 6).
- [Liu 2005]**  
Liu, W. (2005). “Finite Element Modelling of Macrosegregation and Thermomechanical Phenomena in Solidification Processes”. PhD thesis. École Nationale Supérieure des Mines de Paris. URL: <http://pastel.archives-ouvertes.fr/pastel-00001339> (cited on page 9).
- [Martorano et al. 2003]**  
Martorano, M. A. et al. (2003). “A solutal interaction mechanism for the columnar-to-equiaxed transition in alloy solidification”. *Metallurgical and Materials Transactions A*, 34 (8), pp. 1657–1674. URL: <http://link.springer.com/article/10.1007/s11661-003-0311-x> (cited on page 16).
- [Mesri et al. 2009]**  
Mesri, Y. et al. (2009). “Advanced parallel computing in material forming with CIMLib”. *European Journal of Computational Mechanics/Revue Européenne de Mécanique Numérique*, 18 (7-8), pp. 669–694. URL: <http://www.tandfonline.com/doi/abs/10.3166/ejcm.18.669-694> (cited on page 10).
- [Mosbah 2008]**  
Mosbah, S. (2008). “Multiple scales modeling of solidification grain structures and segregation in metallic alloys”. PhD thesis. École Nationale Supérieure des Mines de Paris. URL: <https://tel.archives-ouvertes.fr/tel-00349885/document> (cited on page 9).
- [Ni et al. 1991]**  
Ni, J. and C. Beckermann (1991). “A volume-averaged two-phase model for transport phenomena during solidification”. *Metallurgical Transactions B*, 22 (3), pp. 349–361. URL: <http://link.springer.com/article/10.1007/BF02651234> (cited on page 16).

## Bibliography

---

### [Poirier 1987]

Poirier, D. R. (1987). "Permeability for flow of interdendritic liquid in columnar-dendritic alloys". *Metallurgical Transactions B*, 18 (1), pp. 245–255. URL: <http://link.springer.com/article/10.1007/BF02658450> (cited on page 13).

### [Ramirez et al. 2003]

Ramirez, J. C. and C. Beckermann (2003). "Evaluation of a rayleigh-number-based freckle criterion for Pb-Sn alloys and Ni-base superalloys". *Metallurgical and Materials Transactions A*, 34 (7), pp. 1525–1536. URL: <http://link.springer.com/article/10.1007/s11661-003-0264-0> (cited on page 13).

### [Rappaz et al. 2003]

Rappaz, M. et al. (2003). *Numerical Modeling in Materials Science and Engineering*. Springer Series in Computational Mathematics. Springer Berlin Heidelberg (cited on page 13).

### [Rivaux 2011]

Rivaux, B. (2011). "Simulation 3D éléments finis des macroségrégations en peau induites par déformations thermomécaniques lors de la solidification d'alliages métalliques". PhD thesis. École Nationale Supérieure des Mines de Paris. URL: <http://pastel.archives-ouvertes.fr/pastel-00637168> (cited on pages 9, 17).

### [Sarazin et al. 1992]

Sarazin, J. R. and A. Hellawell (1992). "Studies of Channel-Plume Convection during Solidification". *Interactive Dynamics of Convection and Solidification*. Ed. by S. H. Davis et al. NATO ASI Series 219. Springer Netherlands, pp. 143–145. URL: [http://link.springer.com/chapter/10.1007/978-94-011-2809-4\\_22](http://link.springer.com/chapter/10.1007/978-94-011-2809-4_22) (cited on page 3).

### [Schneider et al. 1997]

Schneider, M. C. et al. (1997). "Modeling of micro- and macrosegregation and freckle formation in single-crystal nickel-base superalloy directional solidification". *Metallurgical and Materials Transactions A*, 28 (7), pp. 1517–1531. URL: <http://link.springer.com/article/10.1007/s11661-997-0214-3> (cited on page 3).

### [Shevchenko et al. 2013]

Shevchenko, N. et al. (2013). "Chimney Formation in Solidifying Ga-25wt pct In Alloys Under the Influence of Thermosolutal Melt Convection". *Metallurgical and Materials Transactions A*, 44 (8), pp. 3797–3808. URL: <http://link.springer.com/article/10.1007/s11661-013-1711-1> (cited on page 3).

### [Tiller et al. 1953]

Tiller, W. A et al. (1953). "The redistribution of solute atoms during the solidification of metals". *Acta Metallurgica*, 1 (4), pp. 428–437. URL: <http://www.sciencedirect.com/science/article/pii/0001616053901266> (cited on page 12).

### [Tourret et al. 2009]

Tourret, D. and C. A. Gandin (2009). "A generalized segregation model for concurrent dendritic, peritectic and eutectic solidification". *Acta Materialia*, 57 (7), pp. 2066–2079. URL: <http://www.sciencedirect.com/science/article/pii/S1359645409000184> (cited on page 16).

**[Wang et al. 1993]**

Wang, C. Y. and C. Beckermann (1993). "A multiphase solute diffusion model for dendritic alloy solidification". *Metallurgical Transactions A*, 24 (12), pp. 2787–2802. URL: <http://link.springer.com/article/10.1007/BF02659502> (cited on page 16).

**[Xu et al. 1991]**

Xu, D. and Q. Li (1991). "Gravity- and Solidification-Shrinkage-Induced Liquid Flow in a Horizontally Solidified Alloy Ingot". *Numerical Heat Transfer, Part A: Applications*, 20 (2), pp. 203–221. URL: <http://dx.doi.org/10.1080/10407789108944817> (cited on page 13).